Front. Phys., 2013, 8(5): 548–554
DOI 10.1007/s11467-013-0371-3

REVIEW ARTICLE

Recent progress in subatomic particle detection technology

Zhi-Huan Li, Jian-Ling Lou, Qi-Te Li, Yu-Cheng Ge, Zhe-Wei Yin, Yan-Lin Ye[†]

School of Physics and State Key Laboratory of Nuclear Physics and Technology, Peking University, Beijing 100871, China

Corresponding author. E-mail: [†]*yeyl@pku.edu.cn*

Received July 28, 2013; accepted August 8, 2013

Particle detection technologies have been largely advanced in our laboratory over the past decade. A neutron sphere was built to detect the decay neutron emitted from the implanted unstable nucleus, whereas a multi-neutron correlation spectrometer was implemented to detect the forward moving neutrons resulting from breakup reactions. Charged particle telescopes are now equipped with double sided Silicon strip detectors which have excellent energy and position resolutions. Large size gas chambers, such as resistive plate chambers, have been developed in order to achieve high performances related to timing or position measurements. The advances of these technologies contribute substantially to such large science project, as LHC-CMS, and to the experiments with the radioactive nucleus beams.

Keywords subatomic particles, detection, nuclear physics

PACS numbers 29.40.Mc, 29.40.Wk, 29.40.Cs, 29.40.Gx

Contents

1 Introduction

Experimental nuclear physics and nuclear physics applications are closely related to particle detection techniques. The particle here has a general meaning, including photons, electrons, muons, pions, nucleons, light and heavy nuclei. Detection is based on using appropriate sensitive materials which interact with the particles and generate corresponding signals. The detectors are therefore classified as scintillation detectors, gas detectors, semi-conducting detectors and so on, according to the active materials used. Each kind of detector has advantages and disadvantages depending on the properties of the particles to be detected. At Peking University the experimental nuclear physics group has developed various particle detection technologies, especially after the establishment of the "Sub-atomic Particle Detection Laboratory" in 1999. At the beginning this lab was created due to the prototyping and mass production of the resistive plate chambers, which is a kind of large size gas detector, to be installed in the large LHC-CMS system dedicated to the detection of the decay products of the Higgs boson and other high energy particles [1, 2]. Later on the requirements from the radioactive ion beam (RIB) physics research have stimulated further development of the laboratory. Until now the lab has greatly expanded and has been equipped with advanced scintillation, gas and Silicon detectors. We give in this article an overview of these detectors and related technologies.

2 Neutron detection

Neutron rich nuclei are of special properties and are now being studied intensively in the literature [3, 4]. Neutron detection with high performance is mandatory in these studies. Neutrons here may be generated in decay or reaction processes. We have built scintillation neutron detectors for both processes [5, 6].

Experimental studies of the β-decay provide rich information on the nuclear structure of the mother and daughter nuclei, especially for nuclei far from the stability line [7, 8]. β-decay of unstable nuclei may release a large amount of energy and can populate the highly ex-

ited states of the daughter nuclide with relatively high probability. The later may emit neutrons or γ-rays which carry rich spectroscopy information of the related systems. Therefore the detection of the decay neutrons with high efficiency and good energy resolution as well as low detection threshold is essential in these decay experiments. At Peking University a decay neutron detection array was built which consists of a neutron sphere and two neutron walls (Fig. 1) [3]. The sphere and the walls are all made of plastic scintillator (BC408). The sphere is composed of eight large-area paddles. Each paddle is a wedge-shaped scintillator with a length of 157 cm and curved to a radius of 100 cm in order to keep the same flight distance for the neutron time of flight (ToF) measurement. The thickness of each paddle is 2.5 cm while the width is 40 cm at the middle but is reduced to 20 cm at both ends. Each end of the scintillator is connected to a photo multiplier tube (PMT) via a light guide of 30 cm long. The sphere covers a solid angle of 30% of 4π sr. The neutron walls include 20 short plastic scintillation bars, each with a length of 40 cm and a cross-section of 4.5×2.5 cm^2. Each end of the bar is connected to a XP2020 PMT via a 10 cm long light guide. The wall is designed to be incorporated inside the sphere, as shown in Fig. 1. Compared to the curved paddles of the neutron sphere, the neutron walls are expected to have higher detection efficiency at low neutron energies due to the lower detection threshold resulting from a smaller size of the scintillator. This performance is crucial for the measurement of low energy neutrons emitted from the energy levels just above the neutron separation threshold of the excited nucleus.

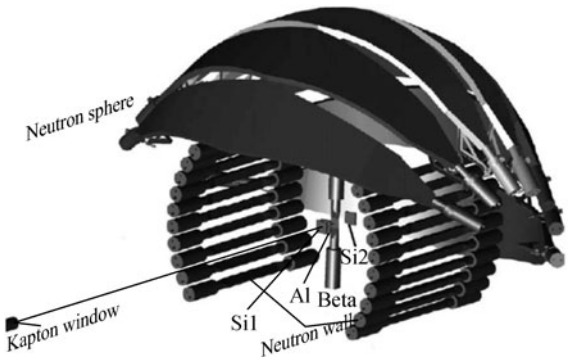

Fig. 1 Schematic view of the β-delayed neutron detection array at Peking University [5].

For a long and wedge-shaped paddle of the neutron sphere, the position resolution is about 10.2 cm (FWHM) at either end of the scintillator and increases to about 14.4 cm (FWHM) at the mid-position of the paddle, based on the test measurement using radioactive sources. For a short bar of the neutron wall, the position resolution is about 3.1 cm (FWHM) and keeps almost constant along the bar. Further investigations were carried out by using accelerated beams of ^{17}N and ^{16}C nuclei, for which the β-delayed neutron emission energies and branching ratios are well known [5]. The energy resolution (Γ) as a function of the incoming neutron energy (E) was obtained from the beam experiment. The relative energy resolution (Γ/E) at 1 MeV is 10.9% for the neutron sphere and 14.7% for the neutron wall, respectively. These resolutions include the uncertainties in determining the ToF and the flight path length. The latter is related to the finite thickness and the inaccurate shape of the scintilator. The intrinsic detection efficiency was also obtained from the beam calibration, as shown in Fig. 2, for the neutron sphere and the neutron wall, respectively. For the neutron sphere, the efficiency rises at energies from 0.383 to 1.17 MeV and then decreases slowly above 1.70 MeV. For the neutron wall, the efficiency is about 36.5% at 1 MeV and keeps a high value at 0.383 MeV (about 26.5%). From the efficiency curve the detection thresholds at low energy side can be set at about 350 keV and 200 keV for the neutron sphere and the neutron walls, respectively. These performances are comparable and even better than similar arrays in other

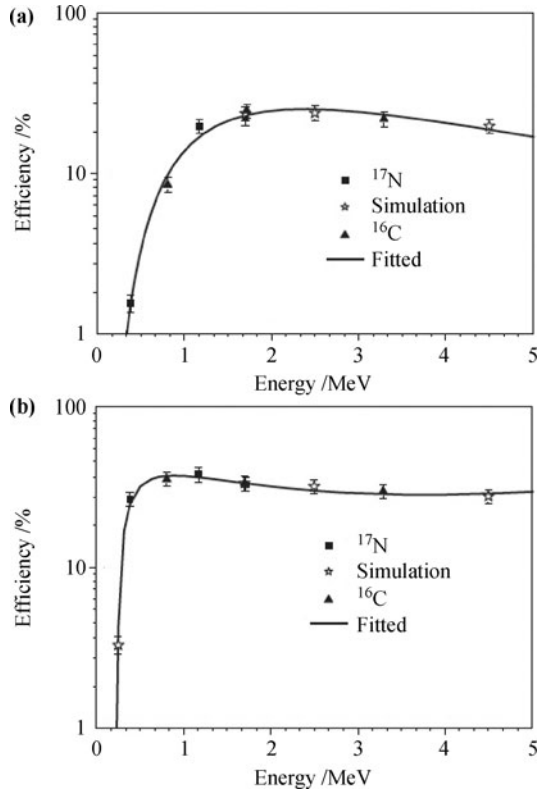

Fig. 2 The intrinsic detection efficiency of the neutron sphere **(a)** and the neutron wall **(b)** as a function of the neutron energy, obtained from the beam test. The solid curves are fitted to the experimental and simulation data points.

labs worldwide.

Owing to the weakly bounding and large size properties of the unstable exotic nuclei, breakup and knockout reactions become powerful tools to study the exotic nuclear structure [9, 10]. Through kinematically complete measurements of reaction products, including the charged core and the valence neutrons (for neutron rich nucleus), spectroscopic information about the internal structure of the exotic nucleus can be extracted. A neutron detector array with good detection efficiency and resolution is mandatory in these studies [6]. In the case of multi-neutron coincidence measurement, the cross talk (CT) rejection is also very important and should be treated carefully [11]. At Peking University we have constructed a Multi-Neutron Correlation Spectrometer (MuNCoS) array, aiming to have a single neutron detection efficiency of about 20% for neutron energies between 10 and 100 MeV, a position resolution of less than 5 cm, and a CT rejection rate of about 90% while retaining about 80% of the detected 2-neutron events.

The MuNCoS consists of 80 scintillation modules (BC-408), each with an active dimension of $200 \times 5 \times 6$ cm^3. In order to discriminate the charged particles that enter the neutron detectors, several thin and large size veto detectors were made, each with a size of $210 \times 35 \times 1$ cm^3 and to be placed in front of any neutron detection layer. Each detector module is wrapped with aluminized Mylar for the internal light reflection and black plastic tape to shield from outside light. A PMT (Hamamatsu R1828-01) is coupled to each end of the module. The whole MuNCoS array can be mounted in various configurations in order to meet specific application goals. Its standard configuration is shown in Fig. 3, including 8 neutron detection layers, each being composed of 10 scintillation modules. There is a gap of about 5 cm between the adjacent two modules in one layer, while the distance between the adjacent two layers is about 50 cm. This scattered configuration is in favor of the CT rejection [11]. From the test with cosmic rays, an average position resolution of about 3.0 cm (FWHM) was obtained for all modules, which is excellent for these large scintillation bars. The neutron detection efficiency of the array was calibrated using neutrons obtained via the (^{11}Be, ^{10}Be+n) Coulomb breakup reaction [6]. The obtained results are shown in Fig. 4. This neutron detection array will play an important role in the studies of the neutron correlation properties in exotic neutron rich nuclei.

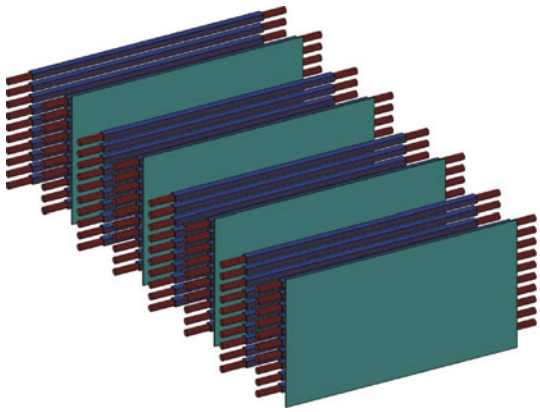

Fig. 3 A schematic view of the MuNCoS array [6].

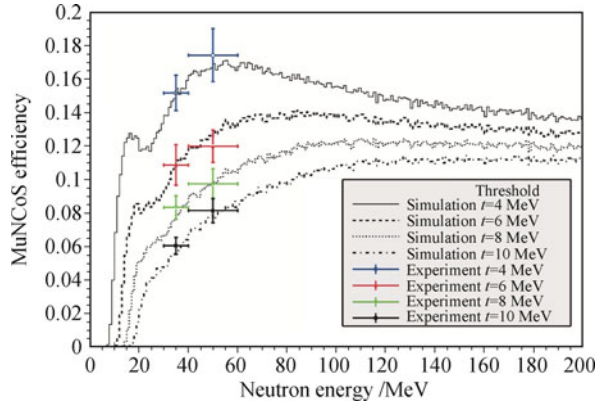

Fig. 4 The experimentally determined neutron detection efficiencies in two energy intervals and at various signal thresholds (*solid dots*), in comparison to the simulated efficiencies (*lines*) [6].

3 Silicon detectors

The energy loss vs. total energy ($\Delta E - E$) telescope has been widely and successfully used to detect the energy and position of the incoming charged particles. It also provides the isotopic particle identification. Many position sensitive telescope arrays have been built in many famous laboratories, such as LASSA [12] and HIRA [13] in MSU, MUST [14] in SACLAY and annular LEAD [15] in Edinburgh and so on. At Peking University, we also begin to construct a telescope array consisting of twelve individual modules, each with a Si-Si-CsI(Tl) configuration. Another two annular silicon arrays are also implemented. The photo views of one typical telescope and one annular silicon array are shown in Fig. 5 and Fig. 6, respectively.

A silicon detector is a reverse-biased diode and often used as the first or second layer in the telescope to record the energy loss of a charged particle. From the single-channel large surface barrier silicon detector (SSD) to the multi-channel position-sensitive silicon detector (PSD), and to the double-sided silicon strip detector (DSSD), the technology has been advanced dramatically during the past decades. With the newly integrated preamplifiers made in our laboratory, a position resolution

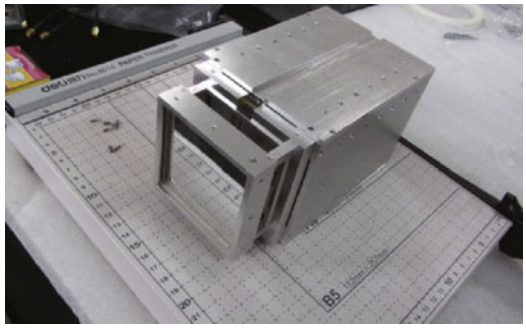

Fig. 5 One typical charged particle telescope.

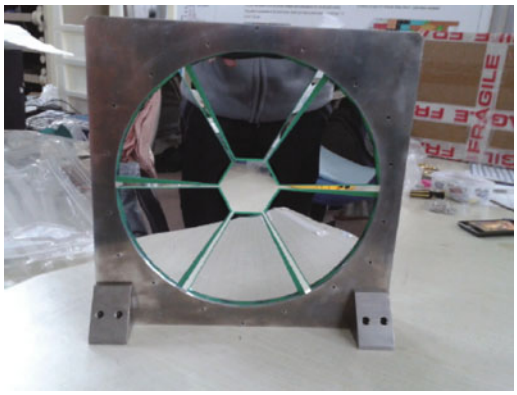

Fig. 6 One annular silicon array.

of less than 2 mm and an energy resolution of 2.1% for 5.486 MeV α particles were obtained for a typical PSD [16]. Generally the DSSD detector has much better position and timing resolutions, and can accept much higher counting rates. However it requires much large number of output channels, each being followed by a costly preamplifier, a shaping-amplifier and some other electronics. We have purchased twelve DSSDs and SSDs produced by Micron company, to be used as the first and second layer of the telescopes. The integrated preamplifiers are made in our lab.

The DSSD has a newly designed BB7 type with an active area of 64×64 mm^2. The strip width is 2 mm at both sides. There are three kinds of thickness for DSSDs, namely 300, 500 and 1000 μm, to be selected for various measurements. The typical energy resolution for 5.486 MeV α particle is about 0.6% for the front side of the DSSD and 0.7% for the rear side, much better than that of the PSD (2.1%). Particles at higher energies will penetrate through the silicon layer, and should be stopped in the CsI(Tl) scintillation counter installed at the back section of the telescope. A configuration of 4×4 modules was adopted for each telescope. Each CsI(Tl) module has a dimension of $4.1 \times 4.1 \times 4.0$ cm^3 and is coupled to a 2.8×2.8 cm^2 pin photodiode. The crystal is individually wrapped with two layers of Tyvek paper inside and several layers of teflon foils outside.

Besides the twelve telescopes, our lab is also equipped with two annular silicon detector arrays. A schematic view of the annular double-sided silicon detector is shown in Fig. 7. One array with a thickness of 150 μm will normally be used as the ΔE detector while the other one with a thickness of about 400 μm could be applied as the E detector. The typical energy resolution for 5.486 MeV α particle is about 0.6% for the front side and 0.7% for the rear side, nearly the same as the above described DSSD.

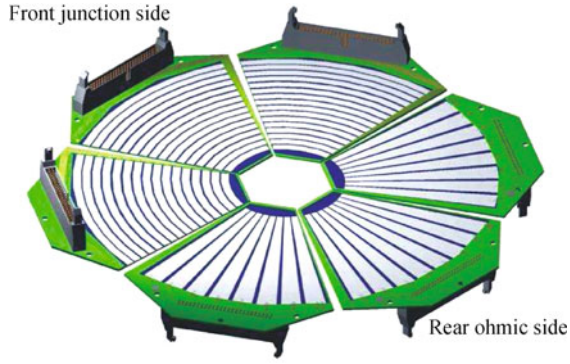

Fig. 7 A schematic view of the annular silicon array.

Some of the telescopes were used in an experiment performed at RIKEN in 2009. The particle identification and the energy resolution were satisfactory [9, 10].

4 Gas detectors

In nuclear and high energy physics experiments, gaseous detectors are very important detection instruments designed to determine trajectory and energy loss of the injected particles. During the last century, different kinds of gaseous detectors were invented and developed for various purposes, such as ionization chambers, proportional counters and Geiger–Müller tubes, and so on. According to our cooperation and experiment need, we have studied several kinds of gaseous detectors in our laboratory, such as avalanche-mode resistive plate chambers (RPCs) made by Chinese materials [17, 18], large area position sensitive resistive plate chambers with delay-line readout [19], low pressure multi-wire proportional chambers(MWPCs) [20] and MWPC with a cathode strip and delay-line readout [21]. Here as examples we focus on the first two types of gas detectors.

4.1 Avalanche-mode resistive plate chambers made by Chinese materials

Resistive Plate Chambers (RPCs) are parallel-plate detectors which were invented around 1980s. Over the

decades, it has been proved that large sized RPCs have many advantages such as a simple and robust structure, long time stability, good time resolution, easy-maintenance and low cost. Large sized RPCs have been widely used in high energy physics experiments [1, 2].

At first, RPCs have been operated in the so-called streamer mode. The large amplitude of the streamer signal allows it to be discriminated without any pre-amplification. The rate capability in this mode is limited (about 100 Hz/cm) because of the long restoration time of the applied voltage after a streamer signal. When the applied high voltage is reduced RPCs can be operated in the so-called avalanche mode. In this mode, only electron propagation is involved in signal formation. The induced signal on the readout strip is small and thus requires front-end amplification. Meanwhile, rate capability in the avalanche mode is increased by more than one order of magnitude. Therefore RPCs working in the avalanche mode are good for high-rate experiments such as CMS at LHC [1, 2].

In order to fully master the RPC technique we have built a prototype RPC by using completely the China-made materials [17, 18]. We compared the surface smoothness of the best bakelite on the international market with specially treated Chinese bakelite which is covered with melamine films. We found that these two kinds of bakelite have similar average roughness value (less than 0.2 um). This assures a significant reduction of the electric background. Bulk resistivity coefficient of the Chinese bakelite is around 5×10^{12} Ωcm.

Figure 8 shows the structure of this RPC prototype. The chamber consists of two gas gaps, each built with two 2 mm thick bakelite plates which form a 2 mm gas gap. The signal pick up layer, located in between of the two gaps, is composed of 32 copper strips. The average width of the strips is 16.3 mm, with a separation of 1.5 mm between two nearby strips. One end of the strip is terminated on a 50 Ω resistor, while the other end is connected to the electronics.

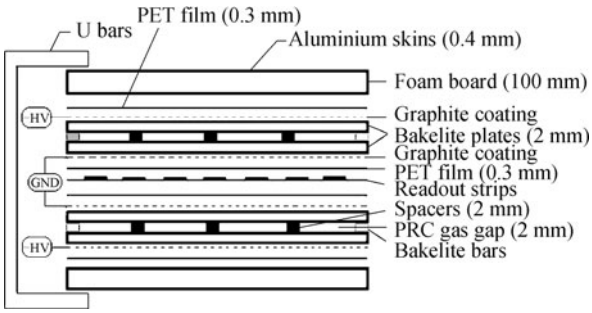

Fig. 8 Cross section view of the double-gap RPC.

This RPC was tested with use of cosmic-ray and 120 GeV/c muon beam at CERN Gamma Irradiation Facility (GIF) [17, 18]. During the cosmic-ray test, avalanche and streamer signals were clearly observed which indicate the correct operation of the chamber. The muon beam test at CERN shows that this RPC worked very well in avalanche mode under standard conditions. The time resolutions get better with increasing high voltages (HV) and reach the minimum of 1–2 ns at HV of 12 kV for all photon rates. As shown in Fig. 9, the RPC reaches full efficiency with a 3000 V wide plateau if the gamma irradiation is canceled. Under higher irradiation rate, the efficiency curve drops down at low voltages. We may estimate that the chamber made up of the Chinese bakelite has a rate capability as high as 400 Hz/cm^2.

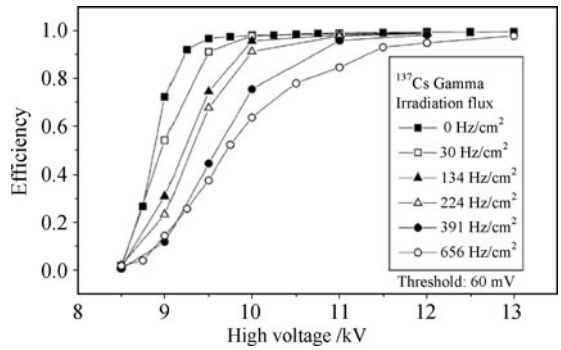

Fig. 9 Efficiency of the home-made RPC as a function of high voltage and gamma irradiation background, and with a discrimination threshold at 60 mV.

4.2 Large area position sensitive RPCs with delay-line readout

In the year 2003, a cosmic muon tomography (MT) method is invented for detecting high Z materials. In order to get a quick and clear MT imaging result, precise measurements of the incoming and outgoing angles of the cosmic muons are crucial. Muon tracking detectors should achieve a sub-millimeter spatial resolution. In the last ten years, some MT facilities using drift tubes, drift chambers and gas electron multiplier detectors have been reported and studied. However, all these detectors have complex structures which will lead to high price. A large number of electronic channels are required as well. In our laboratory, RPC has been well studied and has shown the advantages of simplicity, robustness and low cost. The only problem to be solved is the position resolution [19].

We have carefully chosen the commercial float glass as the resistive electrode of the RPC because its stability, excellent surface smoothness and so on. As shown in Fig. 10, the prototype glass RPC consists of two 2.6 mm thick float-glass plates, each with an area of 30×30 cm^2. The spacers kept precisely a 2 mm gas

gap. The 20×20 cm^2 graphite electrodes were coated on the glass plates for applying HV. 2.54 mm wide readout strips were placed under the glass plates. Mixed gases of $90\%\text{F134a} + 9\%\text{iso} - \text{C}_4\text{H}_{10} + 1\%\text{SF}_6$ were supplied to a gas-tight Aluminum box containing all RPC layers.

The RPCs for MT were tested by using scintillator triggered cosmic rays. Test results showed an detection efficiency for cosmic rays of about 95% for both avalanche and streamer modes of operation [19]. A simple method was developed to measure the induced signal charge profile on readout strips. The measured FWHM of the profile for avalanche signals is about 4 mm, while that for streamer signals is about 12 mm. A narrower profile for avalanche signal mode is certainly in favor of a better spatial resolution [19].

To directly extract the position resolution of the RPC, we adopt an effective approach based on the measurement of all cosmic-ray tracks passing through the whole system with at least three layers of similar detectors [6]. As shown in Fig. 10, three RPCs were symmetrically installed. For each good event, three positions X_1, X_2 and X_3 are recorded from the three RPCs, respectively. The residual can be defined as $\Delta X = X_2 - (X_1 - X_3)/2$. The residual distribution is proportional to the average position resolutions of all three RPCs [6]. The actual FWHM of the residual peak is 1.10 mm, corresponding to an average position resolution (FWHM) of each RPC as 0.9 mm. This test result suggests that the large sized glass RPC in avalanche mode is a promising candidate of the MT detection system.

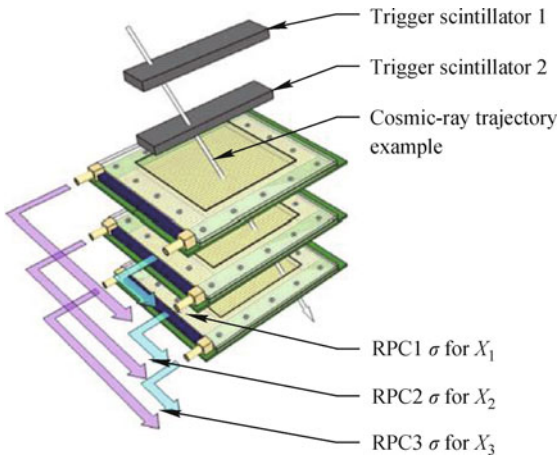

Fig. 10 A schematic view of the detection system composed of three RPCs.

5 Summary

Over the past decade, particle detection technologies have been greatly advanced in our laboratory in order to meet the needs of the nuclear physics experiments, including large neutron detection arrays composed of many plastic scintillation detectors, charged particle telescopes composed of Silicon strip detectors and CsI(Tl) scintillators, and large size gas chambers with excellent timing and position resolutions. Based on these progresses in detection technologies, substantial contributions were made to such international large science project as LHC-CMS. Also the implementation of the new detector arrays has assured the success of the experiments related to nuclear physics far from β stability line.

Acknowledgements Many staffs and students have been involved in the development of the particle detection technology in this laboratory, the contributions of whom are fully acknowledged. The financial support comes from the University and the national funding agencies. This lab is a part of the State Key Laboratory of Nuclear Physics and Technology which provides us with stable operating funding. The current work was supported by the National Basic Research Program of China (973 Program) under Grant No. 2013CB834402 and the National Natural Science Foundation of China under Grant Nos. 11035001, 11275011, and J1103206.

References

1. CMS Collaboration, A new boson with a mass of 125 GeV observed with the CMS experiment at the large hadron collider, *Science*, 2012, 338(6114): 1569
2. CMS Collaboration, Observation of a new boson at a mass of 125 GeV with the CMS experiment at the LHC, *Phys. Lett. B*, 2012, 716(1): 30
3. Z. X. Cao and Y. L. Ye, Study of the structure of unstable nuclei through the reaction experiments, *Sci. China – Phys. Mech. Astron.*, 2011, 54: s1
4. Y. L. Ye and L. H. Lv, Some key problems related to radioactive ion beam physics, *Plasma Science and Technology*, 2012, 14(5): 360
5. J. L. Lou, Z. H. Li, Y. L. Ye, H. Hua, Q. J. Faisal, D. Jiang, X. Li, S. Zhang, T. Zheng, Y. Ge, Z. Kong, Y. Song, L. Lv, C. Li, F. Lu, F. Fan, Z. Li, Z. Cao, L. Ma, Q. Li, and J. Xiao, Performances of a delayed neutron detection array at Peking University, *Nucl. Instrum. Methods A*, 2009, 606(3): 645
6. H. B. You, Z. H. Yang, Y. L. Ye, Z. H. Li, et al., Construction and calibration of the multi-neutron correlation spectrometer at Peking University, *Nucl. Instrum. Methods A*, 2013, 728: 47
7. M. Pfutzner, M. Karny, L. V. Grigorenko, and K. Riisager, Radioactive decays at limits of nuclear stability, *Rev. Mod. Phys.*, 2012, 84(2): 567
8. M. J. Borge, Beta-delayed particle emission, *Phys. Scr.*, 2013, T152: 014013
9. Z. X. Cao, Y. L. Ye, J. Xiao, L. H. Lv, et al., Recoil proton tagged knockout reaction for ^{8}He, *Phys. Lett. B*, 2012,

707(1): 46

10. Y. L. Ye, J. Q. Faisal, J. L. Lou, J. L. GE, Y. C. Lv, L. H. Cao, Z. X. Xiao, J. Li, Q. T. Chen, and T. Y. Yang, Study on structure of unstable nuclei through breakup and knock-out reactions at intermediate and high energies, *Nucl. Phys. Rev.*, 2010, 27: 390
11. H. B. You, Y. S. Song, J. Xiao, and Y. L. Ye, Study of neutron cross talk rejection based on testing experiment and simulation, *Plasma Science and Technology*, 2012, 14(6): 473
12. B. Davina, R.T. de Souza, R. Yanez, Y Larochelle, et al., ASSA: A large area silicon strip array for isotopic identification of charged particles, *Nucl. Instrum. Methods A*, 2001, 473(3): 302
13. M. S. Wallacea, M. A. Famianoa, M. J. van Goethem, A. M. Rogers, et al., The high resolution array (HiRA) for rare isotope beam experiments, *Nucl. Instrum. Methods A*, 2007, 583: 302
14. Y. Blumenfeld, F. Auger, J. E. Sauvestre, F. Maréchal, et al., MUST: A silicon strip detector array for radioactive beam experiments, *Nucl. Instrum. Methods A*, 1999, 421(3): 471
15. T. Davinson, W. Bradeld-Smith, S. Cherubini, et al., Louvain–Edinburgh Detector Array (LEDA): A silicon detector array for use with radioactive nuclear beams, *Nucl. Instrum. Methods A*, 2000, 454(2–3): 350
16. L. Feng, Y. C. Ge, F. Y. Fan, R. Qiao, F. Lu, Y. S. Song, T. Zheng, and Y. L. Ye, Top pair production in the littlest Higgs model with T -parity, *Chinese Phys. C*, 2009, 33(1): 50
17. J. Ying, Y. L. Ye, Y. Ban, H. T. Liu, Z. M. Zhu, Z. Y. Zhu, T. Chen, J. G. Ma, and S. J. Qian, Study of an avalanche-mode resistive plate chamber, *J. Phys. G*, 2000, 26(8): 1291
18. J. Ying, Y. L. Ye, Y. Ban, H. T. Liu, Z. M. Zhu, Z. Y. Zhu, T. Chen, J. G. Ma, and S. J. Qian, Beam test results of a resistive plate chamber made of Chinese bakelites, *Nucl. Instrum. Methods A*, 2001, 459(3): 513
19. Q. T. Li, Y. L. Ye, C. Wen, W. Ji, Y. Song, R. Ma, C. Zhou, Y. Ge, and H. Liu, Study of spatial resolution properties of a glass RPC, *Nucl. Instrum. Methods A*, 2012, 663(1): 22
20. Y. L. Ye, Z. Y. Di, Z. H. Li, Q. J. Wang, T. Zheng, T. Chen, D. X. Jiang, Y. C. Ge, D. Y. Pang, and X. Q. Li, Study and application of low pressure multi-wire proportional chambers, *Nucl. Instrum. Methods A*, 2003, 515(3): 718
21. L. Y. Han, Q. T. Li, Q. Faisal, Y. C. Ge, H. T. Liu, and Y. L. Ye, Study of a multi-wire proportional chamber with a cathode strip and delay-line readout, *Chinese Phys. C*, 2009, 33(5): 364